



## RESEARCH ARTICLE

# Whole-exome sequencing identified five novel *de novo* variants in patients with unexplained intellectual disability

Wenqiu Zhang<sup>1,2</sup>  | Li Hu<sup>2</sup> | Xinyi Huang<sup>3</sup> | Dan Xie<sup>1,2</sup> | Jiangfen Wu<sup>1,2</sup> | Xiaoling Fu<sup>4</sup> | Daiyi Liang<sup>5</sup> | Shengwen Huang<sup>1,2,6</sup> 

<sup>1</sup>School of Medicine, Guizhou University, Guiyang, China

<sup>2</sup>Prenatal Diagnosis Center, Guizhou Provincial People's hospital, Guiyang, China

<sup>3</sup>School of Medical and Life Sciences, Chengdu University of Traditional Chinese Medicine, Chengdu, China

<sup>4</sup>Department of Pediatrics, Guizhou Provincial People's hospital, Guiyang, China

<sup>5</sup>Department of Neurology, Guizhou Provincial People's hospital, Guiyang, China

<sup>6</sup>NHC Key Laboratory of Pulmonary Immunological Diseases, Guizhou Provincial People's Hospital, Guiyang, China

## Correspondence

Shengwen Huang, School of Medicine, Guizhou University, Guiyang 550025, China

Email: [hsw713@sina.com](mailto:hsw713@sina.com)

Daiyi Liang, Department of Neurology, Guizhou Provincial People's hospital, Guiyang, China.

Email: [liangdaiyi@aliyun.com](mailto:liangdaiyi@aliyun.com)

Xiaoling Fu, Department of Pediatrics, Guizhou Provincial People's hospital, Guiyang, China.

Email: [363544564@qq.com](mailto:363544564@qq.com)

## Funding information

Guizhou Science and Technology Projects, Grant/Award Number: 20165670, 20192808 and 20205011; Guiyang Science and Technology Innovation Project, Grant/Award Number: 20161001; Science and Technology Foundation Project of Guizhou Provincial Health Commission, Grant/Award Number: gzwjkj2020-1-250.

## Abstract

**Background:** Intellectual disability (ID) represents a neurodevelopmental disorder, which is characterized by marked defects in the intellectual function and adaptive behavior, with an onset during the developmental period. ID is mainly caused by genetic factors, and it is extremely genetically heterogeneous. This study aims to identify the genetic cause of ID using trio-WES analysis.

**Methods:** We recruited four pediatric patients with unexplained ID from non-consanguineous families, who presented at the Department of Pediatrics, Guizhou Provincial People's Hospital. Whole-exome sequencing (WES) and Sanger sequencing validation were performed in the patients and their unaffected parents. Furthermore, conservative analysis and protein structural and functional prediction were performed on the identified pathogenic variants.

**Results:** We identified five novel *de novo* mutations from four known ID-causing genes in the four included patients, namely *COL4A1* (c.2786T>A, p.V929D and c.2797G>A, p.G933S), *TBR1* (c.1639\_1640insCCCGCAGTCC, p.Y553Sfs\*124), *CHD7* (c.7013A>T, p.Q2338L), and *TUBA1A* (c.1350del, p.E450Dfs\*34). These mutations were all predicted to be deleterious and were located at highly conserved domains that might affect the structure and function of these proteins.

**Conclusion:** Our findings contribute to expanding the mutational spectrum of ID-related genes and help to deepen the understanding of the genetic causes and heterogeneity of ID.

## KEYWORDS

*de novo*, heterogeneity, intellectual disability, variant, whole-exome sequencing

## 1 | INTRODUCTION

Intellectual disability (ID) is a neurodevelopmental disorder that is characterized by marked deficits in the intellectual function and adaptive behavior, which usually develops before the age of 18 years.<sup>1,2</sup> ID has been estimated to have an overall global prevalence of 1%–3%, with a male to female ratio of 1.6:1.<sup>3</sup> This disorder does not only significantly affect the lives of affected children but also their families and society. The etiology of ID is complex and diverse, and it includes different factors, such as genetic abnormalities as well as prenatal, perinatal, and postnatal environmental factors.<sup>4</sup> Previous studies have shown that genetic factors represent major contributors to ID and can explain 25%–50% of the cases. However, this association is complicated by extensive clinical and genetic heterogeneity.<sup>5,6</sup> Therefore, it is essential to perform genetic testing of children with unexplained ID to confirm the diagnosis, select suitable treatment options, and provide genetic counseling to affected families.

Chromosomal abnormalities and single-gene mutations represent important genetic causes of ID.<sup>1</sup> Karyotyping is a traditional and economic approach to diagnose chromosomal anomaly. Regarding single gene mutation, over 800 genes have been so far identified to be involved in the pathogenesis of ID.<sup>7</sup> Mutations in these genes can lead to the disruption of gene co-expression, protein interactions, and related biological functions, which results in ID.<sup>3</sup> Whole-exome sequencing (WES) is based on the next-generation sequencing (NGS) technology and has the advantages of high throughput, accuracy, and speed. In a single step, WES can detect single nucleotide variants (SNVs) and small fragment insertions and deletions (Indels) that are associated with most diseases. This is combined with clinical phenotypic analysis to help clinicians understand the cause of diseases and associated genetic variants, which can effectively improve the diagnosis and shorten the treatment time.<sup>6</sup>

In this study, we conducted WES and identified five novel *de novo* variants from four patients with unexplained ID, in which chromosomal anomaly has been excluded. These variants were all located on known ID-causing genes, namely *COL4A1*, *TBR1*, *CHD7*, and *TUBA1A*. Our findings can expand the mutational spectrum of ID-related genes and deepen our understanding of the genetic causes and heterogeneity of ID.

## 2 | MATERIALS AND METHODS

### 2.1 | Study subjects

This study included four ID patients (under the age of 18 years) from the Department of Pediatrics of Guizhou Provincial People's Hospital. The exclusion criteria included acquired brain lesions or secondary ID, such as ID due to exposure to harmful physicochemical factors during pregnancy, perinatal brain injury, or ID secondary to kernicterus, etc. The study was approved by the Ethics Committee of Guizhou Provincial People's Hospital, and all participants provided written informed consent.

### 2.2 | WES and bioinformatics analysis

Peripheral venous blood samples were collected from all patients and their unaffected parents to perform WES. The steps were briefly as follows. Genomic DNA was extracted from blood samples using the Blood Genomic DNA Kit (TianGen) following the manufacturer's instructions. DNA samples were fragmented to around 200bp using the ultrasonic Bioruptor UCD-200 (Diagenode), followed by DNA library construction using 2×KAPA HiFi HotStart ReadyMix (KAPA Biosystem) and hybridization with whole-exome probes using the xGen Exome Research Panel v1 (IDT). NGS was carried out on a Novaseq6000 Sequencer (Illumina).

Then, we performed the bioinformatics analysis. First, we removed low-quality and adapter reads from raw sequencing data. Then, we used the Burrows–Wheeler alignment (BWA) to align sequencing reads to GRCh37/hg19. Single nucleotide variants (SNVs) and small Indels were identified using SAMtools (v.0.1.18) and GATK (v.3.7–0, <https://www.broadinstitute.org/gatk/>). All detected variants were annotated and classified using the ANNOVAR software. Next, the variants with a minor allele frequency (MAF) > 0.001 in the Genome Aggregation Database (gnomAD) (<http://gnomad-sg.org/>), 1000 Genomes (<http://www.1000genomes.org/>), and ESP6500 (<http://evs.gs.washington.edu/EVS>) were excluded. The variants were subsequently analyzed using independent protein deleteriousness predictors, such as PolyPhen-2 (<http://genetics.bwh.harvard.edu/pph2/>) and SIFT (<http://sift.jcvi.org/>). Finally, we classified the pathogenicity of each genetic variation using Online Mendelian Inheritance in Man (OMIM) (<https://www.omim.org/>), Human Gene Mutation Database (HGMD) (<http://www.hgmd.cf.ac.uk/ac/index.php>), ClinVar database (<https://www.ncbi.nlm.nih.gov/clinvar/>), and the guidelines of the American College of Medical Genetics and Genomics (ACMG) and Association for Molecular Pathology (AMP).<sup>8</sup>

### 2.3 | Sanger sequencing

The mutations identified in the trio-WES and bioinformatics analysis were verified by Sanger sequencing. The primers for polymerase chain reaction (PCR) amplification (Table S1) were designed using Primer 5. All PCR products were sequenced using the ABI 3130 Genetic Analyzer. In order to inspect potential base alterations, sequence analysis was performed using the Chromas program in the DNASTAR analysis package.

### 2.4 | Conservative and in silico analysis

Conservative analysis of the mutant amino acid sequences was performed using the Clustal Omega tool (<https://www.ebi.ac.uk/Tools/msa/clustalo/>). The Phyre2 software (<http://www.sbg.bio.ic.ac.uk/phyre2/html/page.cgi?id=index>) was used to predict the three-dimensional structure and function of the wild-type (WT) and mutant-type (MUT) protein. Then, the Swiss-PdbViewer 4.04

software was used to analyze the structural diversity and physical-chemical changes between WT and related MUT proteins.

### 3 | RESULTS

#### 3.1 | Clinical characteristics of the patients

The four pediatric patients were all born to non-consanguineous parents with no other affected members in their family. The demographic and main clinical characteristics of the four patients are shown in Table S2.

Patient 1 represented a girl aged 1 year and 7 months, and the reason for her visit to the Pediatric Outpatient department was developing “motor development delay, delayed speech and language development and intellectual disability.” According to the fetal period examination, “lateral ventriculomegaly” was indicated. She had a history of asphyxia neonatorum and hyperspasmia the day after birth. Physical examination revealed that her length was 71 cm (−3 standard deviation [SD]), her weight was 7.3 kg (−3 SD), and her circumference of the head was 39.5 cm (−3 SD). The MRI/CT/X-ray implicated tuberous sclerosis. Screening for inherited metabolic diseases was performed and suggested no abnormalities. The Developmental Screening Test (DST) showed a Developmental Quotient (DQ) of 38 and a Mental Index (MI) of 42.

Patient 2 was a girl aged 5 years and 1 month, who visited the Pediatric Outpatient department due to “delayed speech and language development, intellectual disability and autism.” She was unable to run or walk up and down stairs due to muscular hypotonia of the lower limbs. The child was born after a normal gestation without asphyxia or hypoxia. She started walking when she was 1 year and 5 months old, but she had poor balance. Physical examination suggested a length of 112 cm, a weight of 19.3.3 kg (−3 SD) and a head circumference of 50 cm. CMA analysis revealed a partial deletion of 14q11.2, but this fragment lacks the causative genes that are associated with the child's phenotype and is therefore likely a benign variant. The DST showed DQ < 50 and MI < 48.

Patient 3 was a 6-year-old boy with “delayed speech and language development and intellectual disability.” His mother experienced a normal pregnancy, and the baby was born fully developed without asphyxia or hypoxia. Based on the physical examination, his height was 118 cm, and his weight was 29 kg (the head circumference was not available). According to the Wechsler Intelligence Scale for Children, the verbal IQ was 45, and the operational IQ was 48; taken together, his IQ was 42 (moderate).

Patient 4 was a girl aged 2 years and 11 months, who was evaluated for “delayed speech and language development, intellectual disability since birth.” The child could only call “mama” and “papa” and did not speak other words. The mother had a normal pregnancy, and the child was born without asphyxia or hypoxia. She was born with abnormally high muscle tone until the age of one, with poor gross and fine motor development, and she was unable to stand or walk alone. Physical examination revealed a length of 87 cm (−1

SD), a weight of 13.2 kg, and a head circumference of 42 cm (−3 SD). Cranial MRI suggested an absence of the corpus callosum. The DST showed DQ < 48 and MI < 50.

#### 3.2 | Pathogenicity analysis of the five novel mutations

Overall, there were three missense mutations: *COL4A1* (NM\_001845.5: c.2786T>A, p.V929D; NM\_001845.5: c.2797G>A, p.G933S) and *CHD7* (NM\_017780.3: c.7013A>T, p.Q2338L), an insertion mutation: *TBR1* (NM\_006593.3: c.1639\_1640ins CCCGCAGTCC, p.Y553Sfs\*124), and a deletion mutation: *TUBA1A* (NM\_006009.3: c.1350del, p.E450Dfs\*34). All the mutations indicated an autosomal dominant inheritance pattern (Table 1).<sup>9–18</sup>

A compound heterozygous variant c.2786T>A, p.V929D, and c.2797G>A, p.G933S in *COL4A1* was detected in patient 1. According to the OMIM database, mutations in the *COL4A1* gene can cause brain small vessel disease type 1 (BSVD1) with or without ocular anomalies (OMIM: #175780). Both variants were *de novo*, as confirmed by Sanger sequencing (Figure 1A), and absent in the gnomAD and 1000 Genomes Project databases. The results of predicting c.2786T>A and c.2797G>A using SIFT and Polyphen2 showed that they were deleterious. Nucleotide conservation prediction using GERP and CADD showed the site of c.2797G to be evolutionarily conserved with potential functional effects. According to the ACMG/AMP guidelines, the variant c.2786T>A would be classified as likely pathogenic based on the criteria of PS2 and PM2, while the variant c.2797G>A could be classified as likely pathogenic according to the criteria of PS2, PM2, and PP3. Conservative prediction showed the amino acids at positions p.V929 and p.G933 to be highly conserved in nine species (Figure 1B), which suggests that the mutations were likely pathogenic.

In patient 2, we detected a heterozygous insertion variant, c.1639\_1640ins CCCGCAGTCC, p.Y553Sfs\*124 in *TBR1*. According to the OMIM database, this mutation can cause intellectual developmental disorder with autism and speech delay (IDDAS) (OMIM: #606053).<sup>10,11</sup> The variant was confirmed to be *de novo* by Sanger sequencing (Figure 2A) and was absent in the gnomAD and 1000 Genomes Project databases. In this variant, the insertion segment would cause a frameshift mutation, leading to an altered protein function. The ClinGen database showed the haploinsufficiency score of *TBR1* to be 3. According to the ACMG/AMP guidelines, this variant would be classified as pathogenic<sup>8</sup> based on the criteria involving PVS1, PS2, and PM2. Conservative prediction showed that the amino acids at position p.Y553 of *TBR1* were highly conserved in nine species (Figure 2B). According to the three-dimensional structure, the frameshift insertion mutation caused a replacement of tyrosine with serine at position p.553, which would cause the terminal codon to appear in advance, resulting in the production of truncated protein compared with WT. Besides, there was an essential change in the  $\alpha$ -helix in MUT *TBR1*

TABLE 1 Information of the five novel mutations

Patient	Genes	Mutations	Het/Hom	ACMG class and Evidence	Origin and Inheritance patterns	Diseases
1	COL4A1	NM_001845.5: c.2786T>A, p.V929D	Het	LP PS2, PM2	De novo; AD	Brain small vessels disease with or without ocular
		NM_001845.5: c.2797G>A, p.G933S	Het	LP PS2, PM2, PP3	De novo; AD	Anomalies <sup>9</sup>
2	TBR1	NM_006593.3: c.1639_1640insCCCGCAGTCC, p.Y553Sfs*124	Het	P PVS1, PS2, PM2	De novo; AD	Developmental delay with autism and speech delay <sup>10,11</sup>
3	CHD7	NM_017780.3: c.7013A>T, p.Q2338L	Het	LP PS2, PM2	De novo; AD	CHARGE syndrome <sup>12-14</sup>
4	TUBA1A	NM_006009.3: c.1350del, p.E450Dfs*34	Het	LP PS2, PM2	De novo; AD	Lissencephaly-3 <sup>15-18</sup>

Note: The variant interpretation column contains the clinical significance of the variant and the type of evidence supporting the interpretation based on the ACMG/AMP guidelines. Abbreviations: AD, autosomal dominant; Het, heterozygote; Hom, homozygote; LP, likely Pathogenic; P, pathogenic.

protein. The  $\beta$ -pleated sheet and loop were also changed to some extent (Figure 2C, D).

A heterozygous missense variant c.7013A>T, p.Q2338L in CHD7 was detected in patient 3, which would cause the CHARGE syndrome according to the OMIM database (OMIM: #214800).<sup>12-14</sup> Sanger sequencing confirmed this variant to be *de novo* (Figure 3A), and it was absent in the gnomAD and 1000 Genomes Project databases. According to the ACMG/AMP guidelines, this variant would be classified as likely pathogenic based on the criteria involving PS2 and PM2. Conservative prediction showed the amino acid at position p.2338 to be highly conserved in nine species (Figure 3B). According to the three-dimensional structure, when glutamine was replaced by leucine at position p.2338 in CHD7, and although the general structure of the protein did not change (Figure 3C, D), the side chain of the amino acid residues has already changed, as shown in the partial enlargement of the WT and MUT proteins (Figure 3E, F).

As for patient 4, a heterozygous deletion variant c.1350del, p.E450Dfs\*34 in TUBA1A was detected, which would cause lissencephaly-3 (LIS3) according to the OMIM database (OMIM: #611603).<sup>15-18</sup> This variant was *de novo*, as confirmed by Sanger sequencing (Figure 4A) and did not exist in the gnomAD and 1000 Genomes Project databases. According to the ACMG/AMP guidelines, this variant would be classified as likely pathogenic according to the criteria including PS2 and PM2. According to conservative prediction, the glutamic acid at position p.450 in TUBA1A was shown to be highly conserved in nine species (Figure 4B). The three-dimensional structure showed that the frameshift deletion mutation in the MUT protein would skip the original terminal codon, further leading to the production of elongated protein, as compared to the WT (Figure 4B-D).

## 4 | DISCUSSION

In this work, we identified five *de novo* heterozygous pathogenic ID-associated mutations, which have not yet been reported in literature. The mutations included COL4A1 (c.2786T>A, p.V929D and c.2797G>A, p.G933S), TBR1 (c.1639\_1640insCCCGCAGTCC, p.Y553Sfs\*124), CHD7 (c.7013A>T, p.Q2338L), and TUBA1A (c.1350del, p.E450Dfs\*34).

Mutations in the COL4A1 gene cause a variety of diseases, such as retinal artery curvature, vasculopathy and nephropathy, aneurysms and muscle spasm, microvascular disease and cerebral white matter disease with heterogeneity; the effects of mutations in this gene have also been demonstrated in mice.<sup>19-21</sup> COL4A1 encodes a protein that is primarily composed of a repetitive sequence of Gly-Xaa-Yaa, forming a triple helix structure.<sup>22</sup> A previous study on 351 patients with cerebral palsy revealed a strong association between the COL4A1 gene mutations and cerebral palsy.<sup>19</sup> Patients with the c.2699G>A mutation suffer from hemiparesis, epilepsy, cerebral calcification and congenital cataract.<sup>23</sup> As for mutations c.2635G>A, c.2645G>A, c.2654G>A,

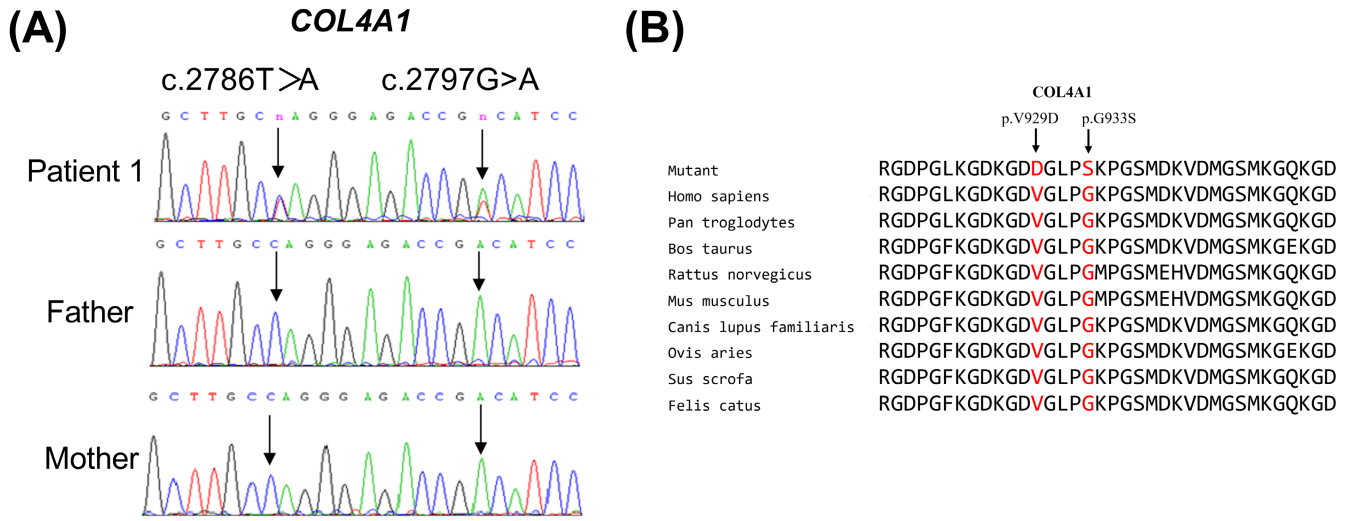


**FIGURE 1** Sanger sequencing and conservative analysis of COL4A1. (A) Sanger sequencing chromatograms show two *de novo* variants in patient 1. Black arrows refer to the mutations; (B) the positions p.V929 and p.G933 in the COL4A1 protein are highly conserved among nine species

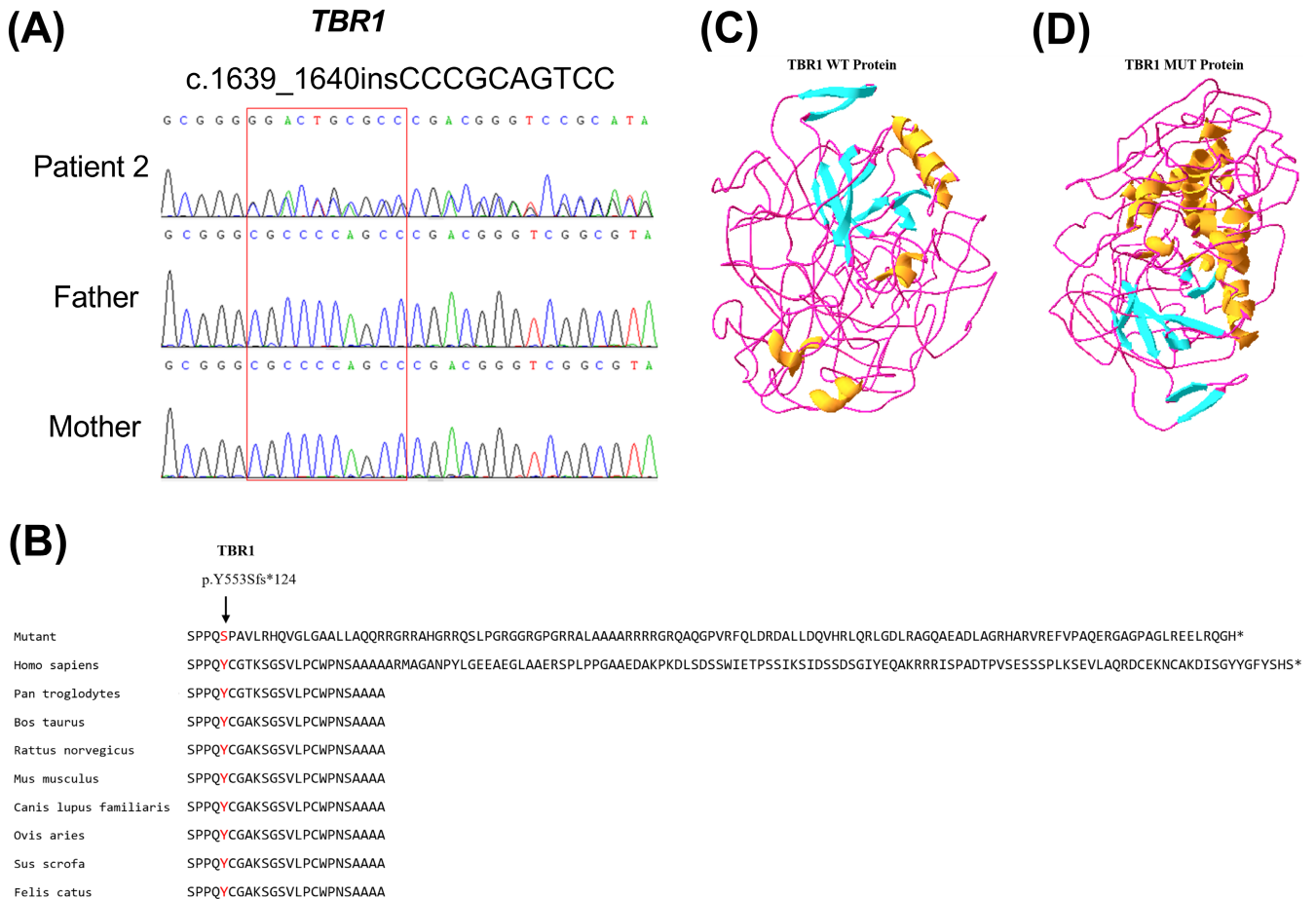


**FIGURE 2** Sanger sequencing, conservative and in silico analysis of TBR1. (A) Sanger sequencing chromatograms show a *de novo* variant in patient 2. The insertion fragment is within a red box; (B) the position p.Y553 residue in TBR1 is highly conserved among nine species; (C, D) the three-dimensional structure prediction of the TBR1 WT and MUT proteins

c.2708G>A, and c.2762G>A, which occurred in the same structural domain with our study, they were all associated with brain lesions.<sup>24</sup> The c.2662G>A mutation results in limb weakness,

developmental delay, seizures, porencephaly, leukoencephalopathy and muscle atrophy, which may be associated with other brain lesions.<sup>25</sup> In our study, the phenotype of patient 1 was similar to

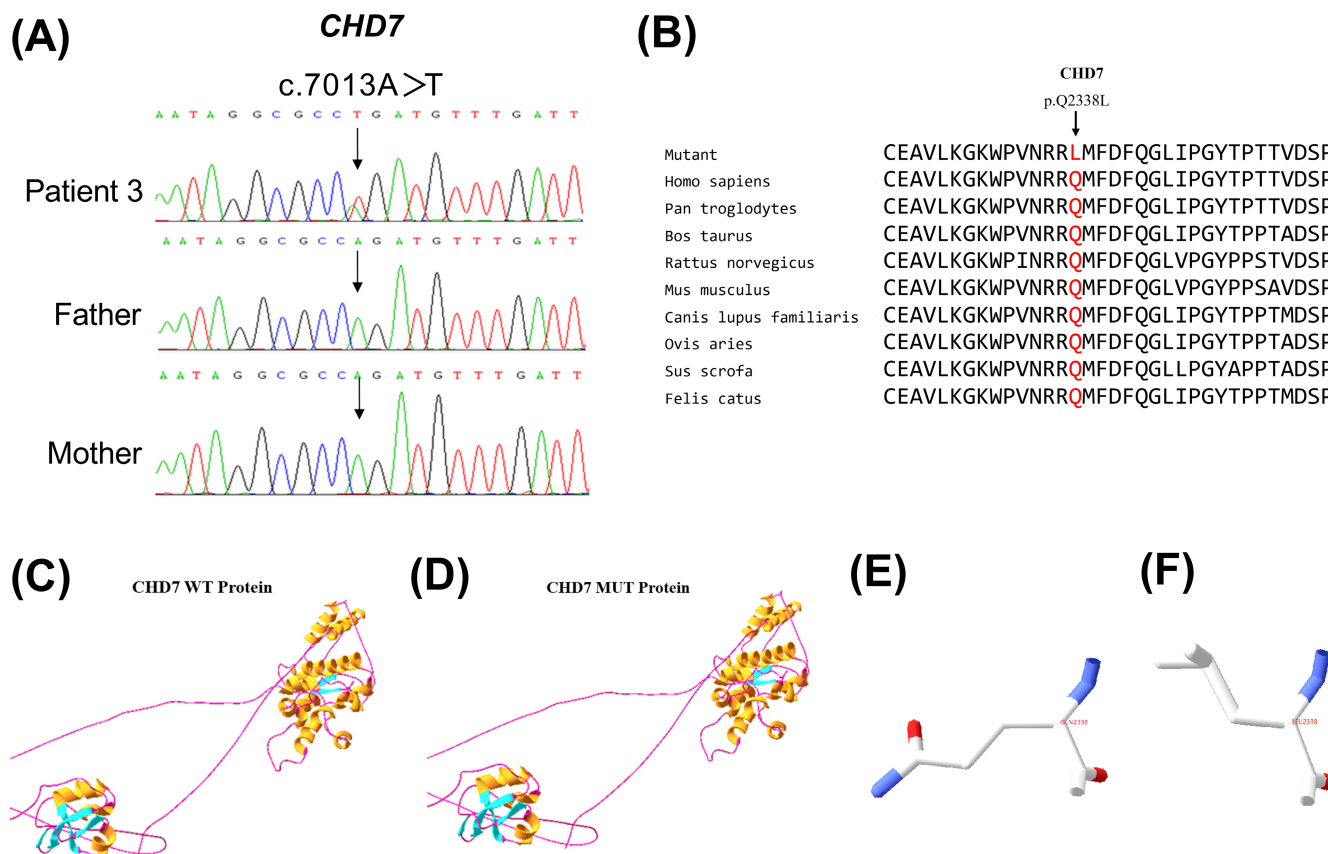


**FIGURE 3** Sanger sequencing, conservative and in silico analysis of *CHD7*. (A) Sanger sequencing chromatograms show a *de novo* variant in patient 3. The black arrow refers to the mutation; (B) the p.Q2338 residue is highly conserved among nine species; (C, D) the three-dimensional structure prediction of the *CHD7* WT and MUT protein; (E) the partial enlargement of the WT *CHD7* protein; (F) the partial enlargement of the MUT *CHD7* protein

that of c.2662G>A. The c.2797G>A mutation results in the protein variant G933S, and the mutation of G in the repeat sequence Gly-Xaa-Yaa may affect the triple helix structure, which impairs the stability of the basement membrane structure and causes the disease.

Autism, delayed language development and intellectual disability are frequently associated with mutations in the *TBR1* gene.<sup>26</sup> In mice, *TBR1* mutations led to the disruption of the activity of neural axons in the amygdala. Furthermore, the mice exhibited decreased social vigor, increased self-cleaning frequency and other anxiety-like behaviors.<sup>27–29</sup> The interaction was revealed between the *TBR1* protein and *FOXP2* protein, which is a transcription factor associated with speech/language disorders, and this interaction could be disrupted by pathogenic mutations in either protein.<sup>10</sup> In this study, the c.1639\_1640insCCCGCAGTCC mutation resulted in a significant structural change in the *TBR1* protein (Figure 2), which may affect the interaction between *TBR1* and *FOXP2*, ultimately resulting in disease development in patient 2. ID and autism are most frequently associated with mutations in the same structural domain.<sup>30</sup> Notably, the c.1588\_1594dup mutation in the same structural domain shares a phenotype with patient 2 and is associated with delayed language development, autism, hypotonia of the lower limbs, and poor limb balance.<sup>31</sup>

*CHD7* mutations are strongly associated with the CHARGE syndrome, which is manifested by eye defects, heart defects, and ear lesions. A survey of 74 patients clinically diagnosed with suspected CHARGE syndrome revealed that 40.5% of them had *CHD7* mutations,<sup>32</sup> while another study on 379 patients revealed that patients with *CHD7* mutations were predisposed to ocular disease and facial developmental disorders.<sup>33</sup> The c.7013A>T mutation was revealed in patient 3, which was not present in any of the general structure, but resulted in an altered side chain structure of the amino acid residues that might affect the protein function (Figure 3). In mice, *CHD7* has been shown to contribute to neurogenesis, and *CHD7* mutant mice were shown to have smaller spiral ganglia and disorganized cochlear neurites. In patient 3 of our study, intellectual disability and language impairment may be associated with their neurodevelopmental disorder. A previous study in Shanghai<sup>36</sup> presented a patient with a *CHD7* mutation, who presented with intellectual disability and hypoplastic laryngeal cartilage, a phenotype similar to that of patient 3 in this study.

*TUBA1A* encodes the tubulin alpha-1A chain, and numerous studies have confirmed an association between *TUBA1A* mutations and brain malformation,<sup>37,38</sup> such that the most common phenotypes associated with these mutations are lissencephaly and polymicrogyria.<sup>39–41</sup> In this study, the c.1350del mutation occurred at the end of the *TUBA1A*

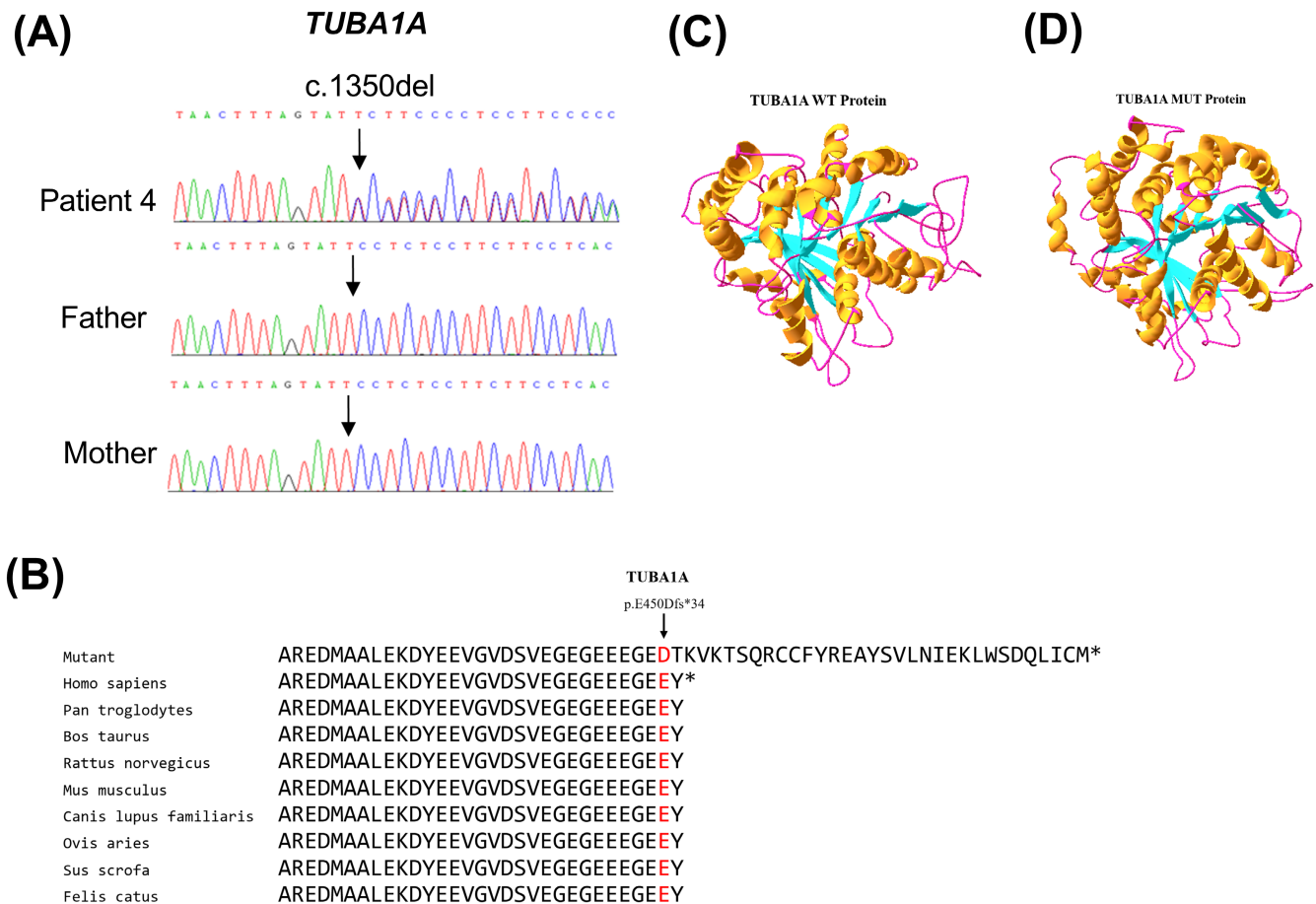


**FIGURE 4** Sanger sequencing, conservative and in silico analysis of *TUBA1A*. (A) Sanger sequencing chromatograms show a *de novo* variant in patient 4. The black arrow refers to the mutation; (B) the position p.E450 in *TUBA1A* is highly conserved among nine species; (C, D) the three-dimensional structure prediction of the *TUBA1A* WT and MUT proteins

gene, which resulted in prolonging the gene and possibly impairing the protein function. Statistical analysis revealed that *TUBA1A* mutations primarily affect the function of the microtubule proteins; while microtubule proteins have some self-repair functions, they are unable to repair the damage caused by the *TUBA1A* mutations, which may be the cause of the c.1350del mutation.<sup>42</sup> Six patients with *TUBA1A* mutations have been described in the literature to have intellectual disability and tetraplegia, which is also consistent with the phenotype of patient 4 in this study, and all six patients were shown to have the *TUBA1A* mutation site in the tail.<sup>17</sup>

One of the limitations of this study is that we did not include functional experiments. Further functional studies either *in vivo* or *ex vivo* are necessary to determine how these five mutations contribute to ID. For example, we can overexpress these five mutations in different specific cell lines or in mice to detect different associated phenotypes.

In summary, by performing WES, we identified five novel *de novo* variants from four patients with unexplained ID. Our findings can expand the mutational spectrum of ID-associated genes and deepen our understanding of the genetic causes and heterogeneity of ID. Further studies are ongoing, aiming to shed light on the pathogenic function of these five mutations in ID.

## ACKNOWLEDGEMENTS

We would like to express our sincere gratitude to all the patients and their families who participated in this study. This work was supported by Guizhou Science and Technology Projects (Grant No. 20165670, 20192808 and 20205011), Guiyang Science and Technology Innovation Project (Grant No. 20161001) and Science and Technology Foundation Project of Guizhou Provincial Health Commission (Grant No. gzwjkj2020-1-250). The authors would also like to express their gratitude to EditSprings (<https://www.editsprings.cn/>) for the expert linguistic services provided.

## CONFLICT OF INTEREST

The authors declare that they have no conflict of interest.

## DATA AVAILABILITY STATEMENT

All the data used to support the findings of this study are included within the article.

## ORCID

Wenqiu Zhang <https://orcid.org/0000-0001-9617-8476>

Shengwen Huang <https://orcid.org/0000-0003-0394-240X>

## REFERENCES

1. Vissers LE, Gilissen C, Veltman JA. Genetic studies in intellectual disability and related disorders. *Nat Rev Genet.* 2016;17:9-18.
2. Agha Z, Iqbal Z, Azam M, et al. Exome sequencing identifies three novel candidate genes implicated in intellectual disability. *PLoS One.* 2014;9:e112687.
3. Kochinke K, Zweier C, Nijhof B, et al. Systematic Phenomics analysis deconvolutes genes mutated in intellectual disability into biologically coherent modules. *Am J Hum Genet.* 2016;98:149-164.
4. Marrus N, Hall L. Intellectual disability and language disorder. *Child Adolesc Psychiatr Clin N Am.* 2017;26:539-554.
5. Liu Z, Zhang N, Zhang Y, et al. Prioritized high-confidence risk genes for intellectual disability reveal molecular convergence during brain development. *Front Genet.* 2018;9:349.
6. Córdoba M, Rodríguez-Quiroga SA, Vega PA, et al. Whole exome sequencing in neurogenetic odysseys: an effective, cost- and time-saving diagnostic approach. *PLoS One.* 2018;13:e0191228.
7. Ben-Mahmoud A, Al-Shamsi AM, Ali BR, Al-Gazali L. Evaluating the role of MAST1 as an intellectual disability disease gene: identification of a novel *De novo* variant in a patient with developmental disabilities. *J Mol Neurosci.* 2020;70:320-327.
8. Richards S, Aziz N, Bale S, et al. Standards and guidelines for the interpretation of sequence variants: a joint consensus recommendation of the American College of Medical Genetics and Genomics and the Association for Molecular Pathology. *Genet Med.* 2015;17:405-424.
9. Gould DB, Phalan FC, van Mil SE, et al. Role of COL4A1 in small-vessel disease and hemorrhagic stroke. *N Engl J Med.* 2006;354:1489-1496.
10. Deriziotis P, O'Roak BJ, Graham SA, et al. *De novo* TBR1 mutations in sporadic autism disrupt protein functions. *Nat Commun.* 2014;5:4954.
11. den Hoed J, Sollis E, Venselaar H, Estruch SB, Deriziotis P, Fisher SE. Functional characterization of TBR1 variants in neurodevelopmental disorder. *Sci Rep.* 2018;8:14279.
12. Oley CA, Baraitser M, Grant DB. A reappraisal of the CHARGE association. *J Med Genet.* 1988;25:147-156.
13. Källén K, Robert E, Mastroiacovo P, Castilla EE, Källén B. CHARGE association in newborns: a registry-based study. *Teratology.* 1999;60:334-343.
14. Tellier AL, Lyonnet S, Cormier-Daire V, et al. Increased paternal age in CHARGE association. *Clin Genet.* 1996;50:548-550.
15. Keays DA, Tian G, Poirier K, et al. Mutations in alpha-tubulin cause abnormal neuronal migration in mice and lissencephaly in humans. *Cell.* 2007;128:45-57.
16. Poirier K, Keays DA, Francis F, et al. Large spectrum of lissencephaly and pachygyria phenotypes resulting from *de novo* missense mutations in tubulin alpha 1A (TUBA1A). *Hum Mutat.* 2007;28:1055-1064.
17. Bahi-Buisson N, Poirier K, Boddaert N, et al. Refinement of cortical dysgeneses spectrum associated with TUBA1A mutations. *J Med Genet.* 2008;45:647-653.
18. Jansen AC, Oostra A, Desprechins B, et al. TUBA1A mutations: from isolated lissencephaly to familial polymicrogyria. *Neurology.* 2011;76:988-992.
19. Bi D, Wang H, Shang Q, et al. Association of COL4A1 gene polymorphisms with cerebral palsy in a Chinese Han population. *Clin Genet.* 2016;90:149-155.
20. Mao M, Smith RS, Alavi MV, et al. Strain-dependent anterior segment dysgenesis and progression to glaucoma in Col4a1 mutant mice. *Invest Ophthalmol Vis Sci.* 2015;56:6823-6831.
21. Colin E, Sentilhes L, Sarfati A, et al. Fetal intracerebral hemorrhage and cataract: think COL4A1. *J Perinatol.* 2014;34:75-77.
22. Weng YC, Sonni A, Labelle-Dumais C, et al. COL4A1 mutations in patients with sporadic late-onset intracerebral hemorrhage. *Ann Neurol.* 2012;71:470-477.
23. Vitale G, Pichiecchio A, Ormitti F, et al. Cortical malformations and COL4A1 mutation: three new cases. *Eur J Paediatr Neurol.* 2019;23:410-417.
24. Itai T, Miyatake S, Taguri M, et al. Prenatal clinical manifestations in individuals with COL4A1/2 variants. *J Med Genet.* 2021;58:505-513.
25. Meuwissen ME et al. The expanding phenotype of COL4A1 and COL4A2 mutations: clinical data on 13 newly identified families and a review of the literature. *Genet Med.* 2015;17:843-853.
26. Chuang HC, Huang TN, Hsueh YP. Neuronal excitation upregulates Tbr1, a high-confidence risk gene of autism, mediating Grin2b expression in the adult brain. *Front Cell Neurosci.* 2014;8:280.
27. Yook C, Kim K, Kim D, et al. A TBR1-K228E mutation induces Tbr1 upregulation, altered cortical distribution of interneurons, increased inhibitory synaptic transmission, and autistic-like behavioral deficits in mice. *Front Mol Neurosci.* 2019;12:241.
28. Huang TN, Hsueh YP. Brain-specific transcriptional regulator T-brain-1 controls brain wiring and neuronal activity in autism spectrum disorders. *Front Neurosci.* 2015;9:406.
29. Huang TN, Chuang HC, Chou WH, et al. Tbr1 haploinsufficiency impairs amygdalar axonal projections and results in cognitive abnormality. *Nat Neurosci.* 2014;17:240-247.
30. Nambot S et al. *De novo* TBR1 variants cause a neurocognitive phenotype with ID and autistic traits: report of 25 new individuals and review of the literature. *Eur J Hum Genet.* 2020;28:770-782.
31. Vegas N, Cavallin M, Kleefstra T, et al. Mutations in TBR1 gene leads to cortical malformations and intellectual disability. *Eur J Med Genet.* 2018;61:759-764.
32. Vuorela P, Ala-Mello S, Saloranta C, et al. Molecular analysis of the CHD7 gene in CHARGE syndrome: identification of 22 novel mutations and evidence for a low contribution of large CHD7 deletions. *Genet Med.* 2007;9:690-694.
33. Zentner GE, Layman WS, Martin DM, Scacheri PC. Molecular and phenotypic aspects of CHD7 mutation in CHARGE syndrome. *Am J Med Genet A.* 2010;152A:674-686.
34. Ohta S, Yaguchi T, Okuno H, Chneiweiss H, Kawakami Y, Okano H. CHD7 promotes proliferation of neural stem cells mediated by MIF. *Mol Brain.* 2016;9:96.
35. Balendran V, Skidmore JM, Ritter KE, et al. Chromatin remodeler CHD7 is critical for cochlear morphogenesis and neurosensory patterning. *Dev Biol.* 2021;477:11-21.
36. Liu L, Yu T, Wang L, Mo X, Yu Y. A novel CHD7 mutation in a Chinese patient with CHARGE syndrome. *Meta Gene.* 2014;2:469-478.
37. Zanni G, Colafati GS, Barresi S, et al. Description of a novel TUBA1A mutation in Arg-390 associated with asymmetrical polymicrogyria and mid-hindbrain dysgenesis. *Eur J Paediatr Neurol.* 2013;17:361-365.
38. Myers KA, Bello-Espinosa LE, Kherani A, Wei XC, Innes AM. TUBA1A mutation associated with eye abnormalities in addition to brain malformation. *Pediatr Neurol.* 2015;53:442-444.
39. Poirier K, Saillour Y, Fourniol F, et al. Expanding the spectrum of TUBA1A-related cortical dysgenesis to polymicrogyria. *Eur J Hum Genet.* 2013;21:381-385.
40. Lecourtis M, Poirier K, Friocourt G, et al. Human lissencephaly with cerebellar hypoplasia due to mutations in TUBA1A: expansion of the foetal neuropathological phenotype. *Acta Neuropathol.* 2010;119:779-789.
41. Hikita N, Hattori H, Kato M, et al. A case of TUBA1A mutation presenting with lissencephaly and Hirschsprung disease. *Brain Dev.* 2014;36:159-162.



42. Aiken J, Buscaglia G, Aiken AS, Moore JK, Bates EA. Tubulin mutations in brain development disorders: why haploinsufficiency does not explain TUBA1A tubulinopathies. *Cytoskeleton (Hoboken)*. 2020;77:40-54.

#### SUPPORTING INFORMATION

Additional supporting information can be found online in the Supporting Information section at the end of this article.

**How to cite this article:** Zhang W, Hu L, Huang X, et al. Whole-exome sequencing identified five novel *de novo* variants in patients with unexplained intellectual disability. *J Clin Lab Anal*. 2022;36:e24587. doi: [10.1002/jcla.24587](https://doi.org/10.1002/jcla.24587)